Title

Volcanic plume height measured by seismic waves based on a mechanical model

Journal

Journal of Geophysical Research, 116(B1)

Authors

Prejean, Stephanie G.
Brodsky, Emily E.

Publication Date

2011-01-26

Peer reviewed

Volcanic plume height measured by seismic waves based on a mechanical model

Stephanie G. Prejean[1] and Emily E. Brodsky[2]

Received 4 April 2010; revised 3 November 2010; accepted 23 November 2010; published 26 January 2011.

[1] In August 2008 an unmonitored, largely unstudied Aleutian volcano, Kasatochi, erupted catastrophically. Here we use seismic data to infer the height of large eruptive columns such as those of Kasatochi based on a combination of existing fluid and solid mechanical models. In so doing, we propose a connection between a common, observable, short-period seismic wave amplitude to the physics of an eruptive column. To construct a combined model, we estimate the mass ejection rate of material from the vent on the basis of the plume height, assuming that the height is controlled by thermal buoyancy for a continuous plume. Using the estimated mass ejection rate, we then derive the equivalent vertical force on the Earth through a momentum balance. Finally, we calculate the far-field surface waves resulting from the vertical force. The model performs well for recent eruptions of Kasatochi and Augustine volcanoes if v, the velocity of material exiting the vent, is 120–230 m s^{-1}. The consistency between the seismically inferred and measured plume heights indicates that in these cases the far-field ~1 s seismic energy radiated by fluctuating flow in the volcanic jet during the eruption is a useful indicator of overall mass ejection rates. Thus, use of the model holds promise for characterizing eruptions and evaluating ash hazards to aircraft in real time on the basis of far-field short-period seismic data. This study emphasizes the need for better measurements of eruptive plume heights and a more detailed understanding of the full spectrum of seismic energy radiated coeruptively.

Citation: Prejean, S. G., and E. E. Brodsky (2011), Volcanic plume height measured by seismic waves based on a mechanical model, *J. Geophys. Res.*, *116*, B01306, doi:10.1029/2010JB007620.

1. Introduction and Motivation

[2] Empirical studies have suggested that the amplitude of high-frequency or broadband seismic waves radiated during large volcanic eruptions generally scales with the height of an eruption column [*McNutt*, 1994a]. However, a direct calculation of the expected seismic wave amplitude based on physical models has not yet been successful. Connecting commonly observable data such as seismic wave amplitudes to a model of the flow in the eruptive jet would provide a new tool to test and improve our understanding of eruptive physics. For instance, small-scale turbulence is thought to play a major role in the entrainment of hot particles and gases and hence the buoyancy of eruptive columns, yet there are few measurements of the strength or distribution of small-scale features in real eruptive columns [*Andrews and Gardner*, 2009]. Using seismic data to provide observational constraints on eruption column flow processes is particularly attractive as seismic data are often available even in remote settings. Thus use of the seismic database would greatly increase the number and type of eruptions amenable to study.

[3] Pragmatically, a physical model connecting plume height and seismic data would allow the use of seismology as a remote sensing technology to infer volcanic plume height. It would be a particularly useful tool for exploring eruption dynamics in remote environments where direct observation is not possible, such as the volcanoes of the northern Pacific Ocean. Although many volcano observatories worldwide are gradually replacing short-period seismometers with broadband seismometers, we still largely rely on short-period instruments for forecasting, monitoring, and analyzing eruptions. These realities motivate the development of the model described below.

[4] In this study, we build on previous work to develop a physical model for the expected amplitude of seismic waves from an eruption that generates a plume of a given height. As a cautionary note, we explore the potential errors in this formulation and describe situations where the model is not applicable, such as small eruptions or eruptions where most mass ejected is not entrained in the plume. After reviewing previous work on coeruptive seismology and the characteristics of the 2008 Kasatochi and 2006 Augustine eruptions, we use the connection between plume height and

[1] U.S. Geological Survey, Alaska Volcano Observatory, Anchorage, Alaska, USA.
[2] Department of Earth and Planetary Sciences, University of California, Santa Cruz, California, USA.

0148-0227/11/2010JB007620

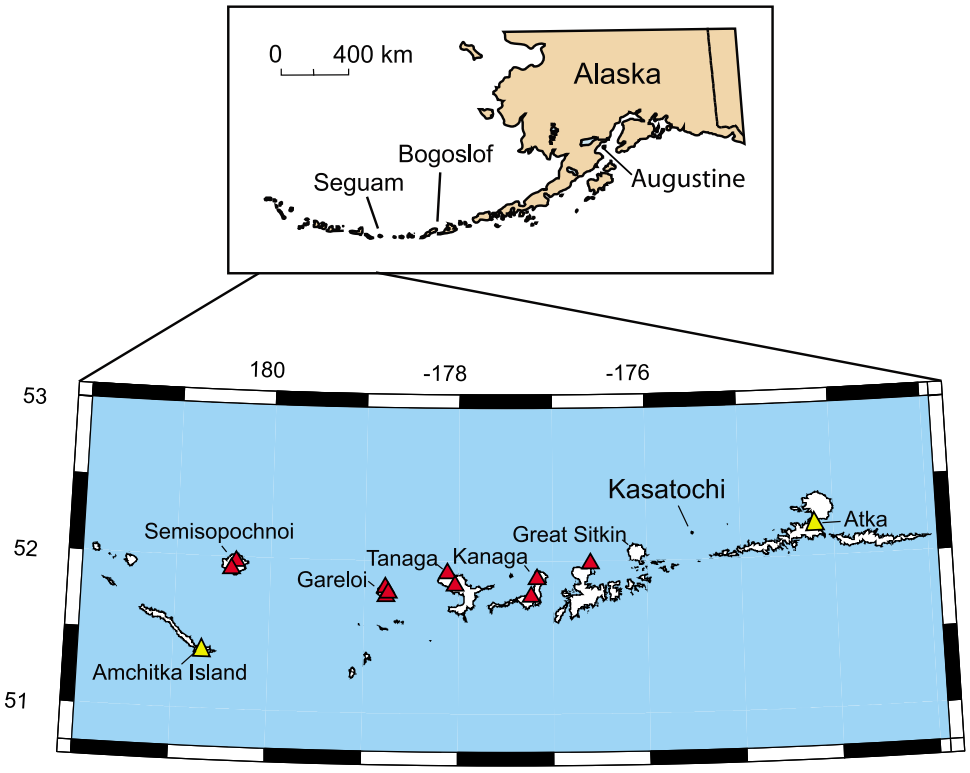

Figure 1. Map of the central Aleutian arc showing locations of Augustine Volcano, Kasatochi Island, and neighboring islands and volcanoes. Seismic stations used in this study are indicated by triangles. Red triangles are short-period instruments. Yellow triangles are broadband instruments. Great Sitkin Volcano had a functioning seismic network at the time of the Kasatochi eruption. However, those data were clipped and not used in this study.

thermal ejection rate to predict the momentum ejection rate that generates the seismic waves. We then compare the model to data for the eruptions of Kasatochi and Augustine volcanoes and show that, for a reasonable range of parameters, the model performs well.

2. Background

2.1. Coeruptive Seismology

[5] Volcanic activity produces seismic waves. These waves, which include brittle failure earthquakes, long-period and very long period events, and volcanic tremor, generally result from movement of fluid in the Earth's subsurface, directly and indirectly (see *Chouet* [1996] and *McNutt* [2005] for reviews). Seismology also directly senses magma leaving the Earth in the form of both eruption tremor and discrete eruption earthquakes [e.g., *Nishimura and Hamaguchi*, 1993; *Nishimura*, 1995]. Such coeruptive seismicity has been documented in the scientific literature since *Omori*'s [1911] early studies of Usu-san and Asama volcanoes and is the subject of this study.

[6] By analyzing long-period surface waves radiated by the 18 May 1980 eruption of Mount St. Helens, *Kanamori and Given* [1982] show that the coeruptive seismic source can be represented kinematically by a near-vertical downward single force. This single force represents the counterforce of eruption [*Kanamori et al.*, 1984]. This model has been used to investigate eruption source properties of volcanic eruption earthquakes at other volcanoes, including Mount Tokachi and Mount Asama, Japan [*Nishimura*, 1995; *Nishimura and Hamaguchi*, 1993; *Ohminato et al.*, 2006]. *Brodsky et al.* [1999] calculated vertical mass discharge rates for the 18 May 1980 eruption of Mount St. Helens on the basis of this model. Our work follows these studies.

[7] Other models for the source of coeruption seismicity exist. For example, *Uhira and Takeo* [1994] showed that in the case of the 1986 eruptions of the Sakurajima Volcano in Japan, a single force model cannot explain long-period (several seconds) seismic radiation patterns as well as a model containing volumetric components of expansion and contraction of rock around the source. *Chouet et al.* [2010] show that in the case of the Kilauea Volcano, explosive degassing bursts associated with Strombolian eruptions are complex and best modeled by a combination of single-force and volumetric changes at low frequencies in conjunction with higher-frequency oscillations in the conduit and short-period energy from the slug burst itself. Additional studies also find source mechanisms consisting of single force components and volumetric change, such as those at Stromboli and Popcatepetl [*Chouet et al.*, 2003, 2005, 2008].

[8] Overall, the source of low-frequency energy radiated coeruptively has been more thoroughly studied than high-frequency energy radiated coeruptively. *McNutt and Nishimura* [2008] model coeruptive tremor as resulting

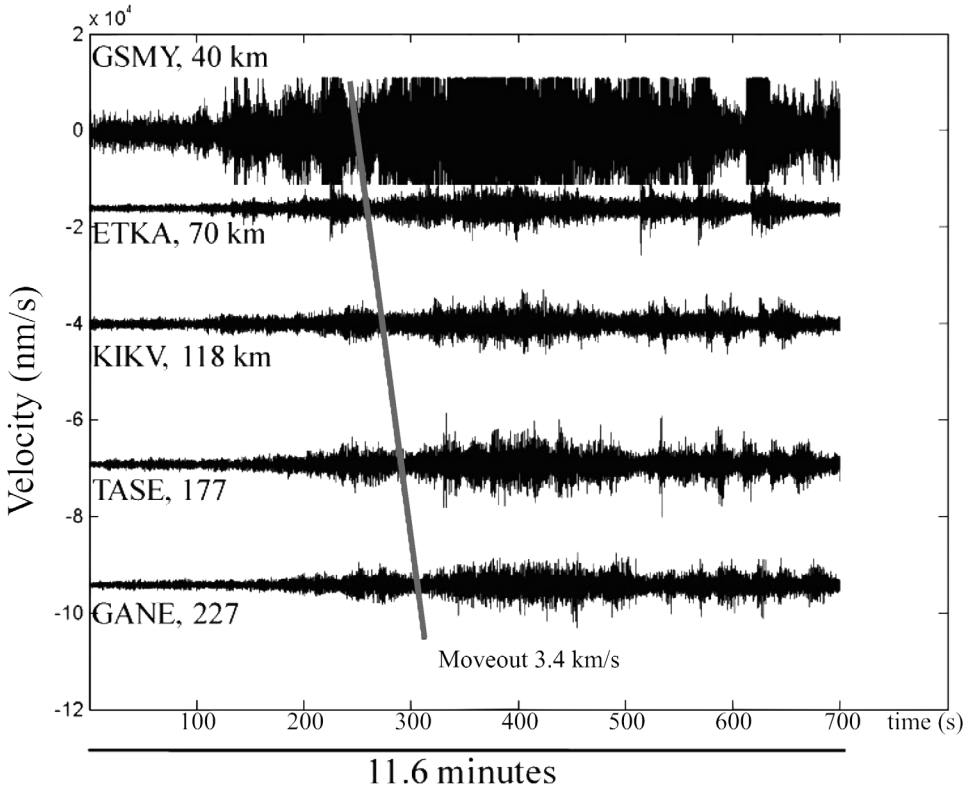

Figure 2. Raw waveform of third ash-producing explosion of Kasatochi as recorded on short-period stations GSMY, ETKA, KIKV, TASE, and GANE. Shaded line shows moveout of surface wave energy packets at 3.4 km s^{-1}.

from radial oscillations of conduit walls but do not connect the amplitudes to the plume dynamics. Here we take a different approach and model the seismic wave generation as resulting from the mass discharge of the erupting column.

2.2. The 2008 Eruption of Kasatochi Volcano

[9] Kasatochi Volcano is a 3 km wide island with a large crater lake in the Andreanof Islands in the Aleutian Arc (Figure 1). Though the volcano's summit is 314 m in elevation, the volcanic vent is near sea level. Prior to its 2008 eruption, little was known about this volcano. Kasatochi Volcano is not seismically or geodetically monitored. The nearest seismometers are a short-period network operated by the Alaska Volcano Observatory (AVO) at Great Sitkin Volcano, 40 km west of Kasatochi (Figure 1). The nearest broadband station functioning at the time of the eruption, ATKA operated by the Alaska Earthquake information Center (AEIC), is 80 km east of Kasatochi on Atka Island.

[10] After a brief but powerful earthquake swarm with earthquakes as large as M_W 5.8 [*Ruppert et al.*, 2011], Kasatochi Volcano had three large ash-producing eruptions with satellite detectable plumes to 18 km above sea level (2201 UTC on 7 August 2008, 0150 and 0435 UTC on 8 August 2008) [*Waythomas et al.*, 2010]. Maximum heights reported correspond to the plume top rather than the umbrella cloud. Coeruptive tremor associated with each of these three explosions was readily apparent in real-time seismic data for at least 20 min (Figure 2). Infrasound and seismic data indicate that two additional smaller explosions occurred in the following 5 h episode of continuous ash emissions [*Arnoult et al.*, 2010]. Satellite data indicate that the third large explosion was significantly more ash-rich and had a higher plume than the first two explosions [*Waythomas et al.*, 2010; *Fee et al.*, 2010; *Scott et al.*, 2010]. Seismic data support this observation as the far-field amplitude of the third explosion was more energetic than the previous explosions. Following the third explosion, ash vented continuously for roughly 16 h. Satellite data indicate that the continuous ash emission phase had a decreasing density of ash emission with time [*Waythomas et al.*, 2010]. This observation is consistent with seismic data, as the prolonged continuous ash emission phase radiated less seismic energy than the initial 10 min of the third explosion.

2.3. The 2006 Eruption of Augustine Volcano

[11] The 2006 eruption of Augustine Volcano was far better monitored than the 2008 eruption of Kasatochi, in part because the volcano had erupted previously in 1971, 1976, and 1986. Augustine, a volcano located in the lower Cook Inlet with summit at 1260 m above sea level (Figure 1), is instrumented with both broadband and short-period seismometers. Increasing seismicity and deformation were noted months before the eruption onset [*Power and Lalla*, 2010]. The Augustine preeruptive seismic swarm was notably less intense than that of Kasatochi. The largest earthquake associated with the eruption was M_L 2.1. The explosive

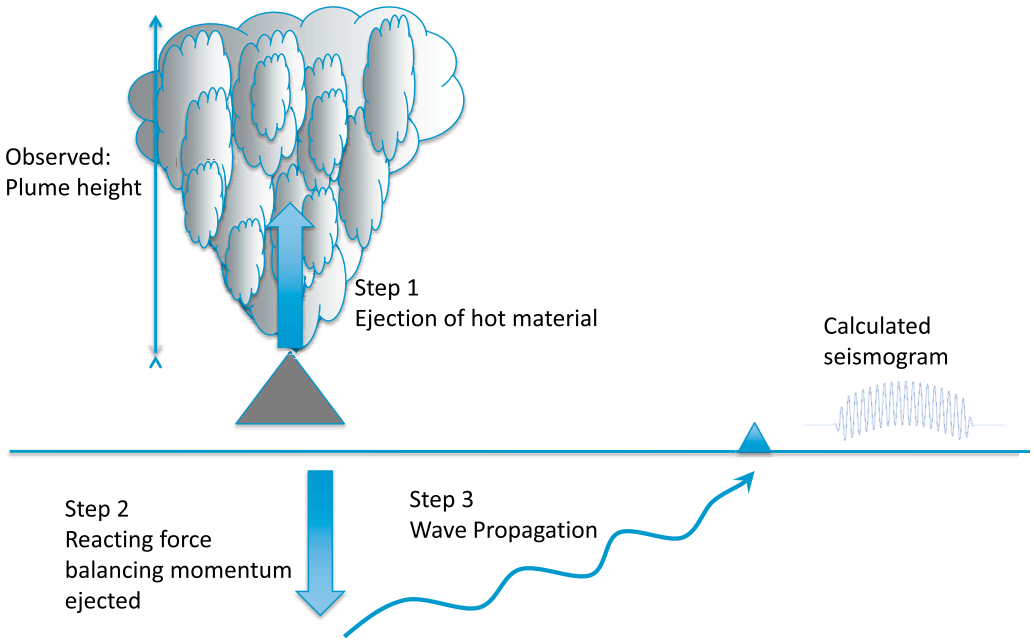

Figure 3. Cartoon depicting processes associated with the three calculation steps in the composite model. Step 1 relates plume height to mass ejection rate. Step 2 relates mass ejection rate to a downward acting single force. Step 3 calculates seismic waves radiated by the single force. Calculated seismic wave amplitudes are compared to those observed.

phase of the eruption began on 11 January 2006 and continued through 28 January 2006 [see *Power and Lalla*, 2010]. The ash-producing explosions of Augustine, though numerous, were shorter in duration and lower in altitude than the Kasatochi explosion. Augustine produced 13 major ash plumes ranging in altitude from 9 to 14 km above sea level. The coeruptive tremor durations for these explosions, as determined from far-field seismic data, ranged from 3 to 7 min. The coeruptive seismicity associated with the Augustine eruption plumes was observed at a maximum distance of ~200 km, whereas Kasatochi coeruptive seismicity was visible to over 350 km distance.

3. Relating Plume Height to Seismic Wave Amplitudes

[12] Here we develop a composite model that combines existing fluid and solid mechanical models to connect observable seismic wave amplitudes to volcanic plume height. We test the model on the 2008 eruption of Kasatochi Volcano and the 2006 eruption of Augustine Volcano. The model involves three distinct steps as illustrated in Figure 3: (1) Relate maximum ash plume height to mass ejection rate of material from the volcanic vent. (2) Relate mass ejection rate to a single downward force acting on the solid Earth. (3) Calculate far-field seismic wave amplitudes resulting from the single force. Each step is described in detail below.

3.1. Step 1: Relate Plume Height to Mass Ejection Rate

[13] We begin by assuming that plume height is controlled by thermal buoyancy for a continuous ash-rich plume with dense rock equivalent volumetric ejection rate q. This fundamental physics for column height has its origins in studies of forest fire plumes [*Morton et al.*, 1956] and has been verified using eruption data [*Carey and Sigurdsson*, 1989; *Sparks et al.*, 1997]. Slightly different relationships between q and plume height exist in the literature, depending on the data sets used for calibration. We use the widely cited *Sparks et al.*'s [1997] equation 5.1:

$$H = 1.67\, q^{0.259}, \tag{1}$$

where q is in $m^3\ s^{-1}$ and H is the maximum column height in km above the vent rather than the sometimes more easily observed height of the umbrella cloud. Equation (1) is an empirical regression, but its form is motivated by analytic models of thermally buoyant continuous plumes in a stratified atmosphere [*Sparks et al.*, 1997, equation 4.15; *Wilson et al.*, 1978]. Observations used to constrain equation (1) include uncertainties both in plume height and in ejecta volumes as discussed by *Mastin et al.* [2009] and *Sparks et al.* [1997]. We use the term *continuous* to describe a plume where the volcano is still actively venting at the time the plume reaches its maximum height. This is often referred to as an *attached plume*.

[14] An alternative model is a rapid ejection eruption where all of the mass is released so quickly that the bottom of the plume has left the vent before the top of the plume reaches its maximum height. Though this may have been the case for the first two Kasatochi explosions, satellite data show that this was not likely the case for the third explosion, as that explosion was the beginning of a 13 h phase of continuous ash emission [*Waythomas et al.*, 2010]. Nonetheless, it is useful to realize that even in this case, the scaling in equation (1) is preserved and the only major modification is the inclusion of the ejection duration.

Morton et al. [1956] also developed a relationship for a quickly released plume and found

$$H = 1.87 \times 10^{-3}\, E^{1/4}, \quad (2)$$

where H is height in km and E is thermal energy in J. The thermal energy is primarily carried by the solid particles, and $E = c_p\, \rho\, \Delta T\, q\, \tau$, where c_p is the heat capacity, ρ is the density of the solid rock, ΔT is the temperature difference between the plume and the ambient air, and τ is the duration of the ejection phase. Using reasonable values for parameters (c_p = 1 kJ kg^{-1} K^{-1}, ρ = 3000 kg m^{-3}, ΔT = 10^3 K, τ = 100 s) yields

$$H = 1.4\, q^{1/4}, \quad (3)$$

which is consistent with the empirical protracted source result (equation (1)). Thus, the model is insensitive to the assumed relative duration of the source.

[15] We next relate the volumetric ejection rate to the mass ejection rate, as the later quantity is most directly associated with the momentum flux which ultimately generates seismic waves. If dense rock equivalent density is ρ, then

$$\dot{M} = q\rho, \quad (4)$$

where $\dot{M}$ is the mass ejection rate.

3.2. Step 2: Relate Mass Ejection Rate to Single Force

[16] We assume that the force system acting on the Earth during an eruption can be represented as a single force following the work by *Kanamori and Given* [1982], *Kanamori et al.* [1984], and *Brodsky et al.* [1999]. Owing to a lack of quality broadband seismic data and poor coverage of the focal sphere typical of Aleutian eruptions, we are not able to invert the coeruptive seismic radiation field of the Kasatochi eruptions for an equivalent force system. Thus, we cannot directly demonstrate that a single force is the most appropriate source model for Kasatochi. Instead, we start with this simple seismic source model and test its applicability.

[17] Using the mass ejection rate from equation (4), we can derive the equivalent vertical force F on the Earth using a momentum balance following *Brodsky et al.* [1999]:

$$d(\text{Momentum})/dt = \dot{M}\, v = F, \quad (5)$$

where v is the velocity of material exiting the vent. This is sometimes termed the *thrust equation* [*Thompson*, 1972]. In the case of a rocket, the force propelling a rocket upward is equal to the momentum discharge rate of the fuel behind it. In the case of a volcano, the rocket is inverted, as it discharges momentum upward. Equation (5) is a quasi-static approximation that assumes that the advective transport of momentum is more significant than the local acceleration. For any protracted plume source, this is likely appropriate.

[18] As $\dot{M}$ also depends on the vent velocity v through the volumetric flow rate q, equation (5) can be expanded using equation (4) and the definition of volumetric flow rate at the vent ($q = vA$, where A is the area of the vent) to show that the force F is proportional to v^2. However, it is more useful to keep the form of equation (5) as written above, as this form minimizes the number of unconstrained parameters, since the observable column height H is a function of the combined quantity q. Using this combination of parameters introduces an important and subtle assumption about the frequency content of the observations used to estimate q and v that is discussed below.

[19] To use equation (5), we need to estimate only one unknown parameter, v. For large-scale eruptions, the extreme overpressures at the vent require supersonic flow. In steady state, the flow is choked at the vent with the vent velocity equal to the sound speed of the erupting material [*Kieffer*, 1981; *Woods*, 1995]. The mixture of ash and gas in a plume has a greatly depressed sound speed relative to either the solid or gas end-member [*Rudinger*, 1980]. For instance, the 18 May 1980 blast of Mount St. Helens is thought to have had a sound speed of ~100–250 m s^{-1} on the basis of the temperature and relative mass fraction of gas and solid phases [*Kieffer*, 1981; *Brodsky et al.*, 1999]. Alternative derivations of the vent velocity on the basis of conduit flow models also arrive at the same range of 100–250 m s^{-1} [*Papale and Longo*, 2008]. *McNutt and Nishimura* [2008] summarized vent velocity estimates for a large number of eruptions globally and arrived at a range of 28–420 m s^{-1} with the caveat that the lowest end of the range is likely an underestimate due to the neglect of the coupled gas flow. We consider vent velocities within both the observational and theoretical ranges (100–250 m s^{-1}) reasonable and consistent with prior work.

[20] The simplest application of equation (5) would be using data with periods of minutes, consistent with the time it takes to evacuate the magma chamber, following *Kanamori et al.* [1984]. This approach would be consistent with the duration of the observations used to constrain q from the column height. We lack seismic data at those frequencies, so we explore the possibility that the higher-frequency seismic waves radiated by turbulence in the volcanic jet scale with energy radiated at low frequencies. To provide the context for this approach, we now discuss the role of turbulence in the volcanic jet.

[21] The observed spectrum of seismic waves is a product of the propagation spectrum in the elastic medium (see equation (6) below) and the spectrum of momentum ejection from the vent (source spectrum). The spectrum at the source may primarily reflect the spectrum of vent velocities. In a turbulent flow, fluid velocity generally fluctuates with well-defined statistical properties. For instance, for homogeneous, isotropic turbulence in an incompressible flow, the energy spectrum, S, of the flow is related to frequency $S \sim f^{-5/3}$ [*Kolmogorov*, 1941; *Mathieu and Scott*, 2000]. A volcanic eruption involves transient, compressible flow that has multiple origins of velocity fluctuations, including the turbulent field, internally generated periodic collapses, and evolving vent shape [*Ogden et al.*, 2008]. For simplicity, in this initial study, we assume that the vent velocity spectrum is flat and that the spectral amplitude is v for all frequencies. We also do not consider here the influence of density fluctuations on the source spectrum. This flat spectrum assumption allows us to use equation (5) with $\dot{M}$ estimated from the column height and v estimated separately on the basis of the seismic waves. These assumptions are difficult to evaluate in the absence of direct observations of the turbulent structure of plumes and

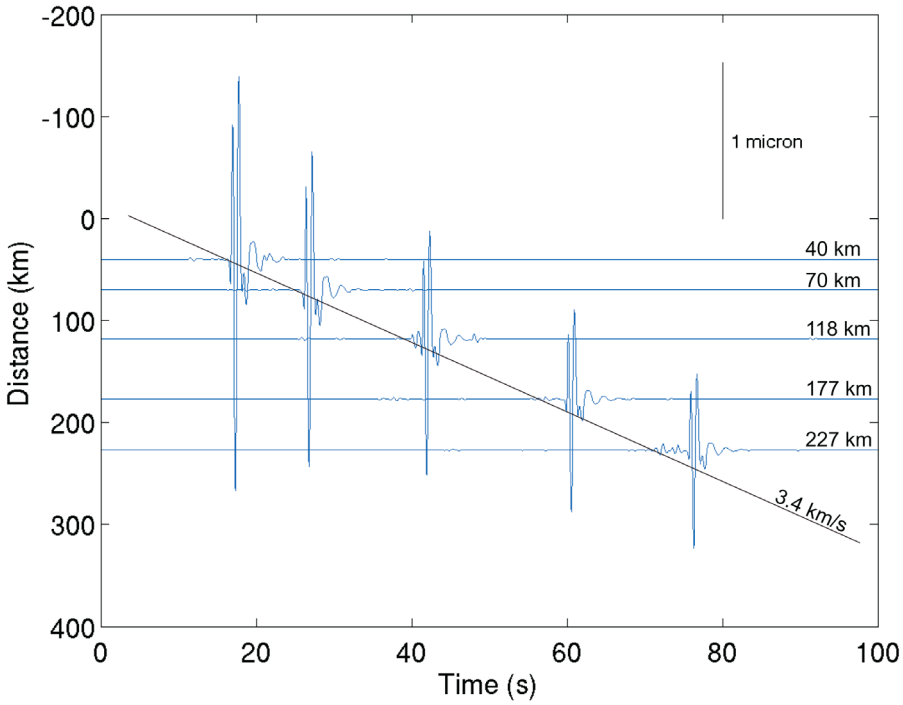

Figure 4. Synthetic seismograms from an impulse source of the same strength as that inferred for the Kasatochi eruption. The synthetics are band passed using the same filter as the observed seismograms (0.67–2 s) to measure the amplitude in the narrow band pass corresponding to equation (7). The synthetics were produced using a regional f-k integration and the AK135 model [*Kennett et al.*, 1995; *Montagner and Kennett*, 1996; R. B. Herrmann, Computer programs in seismology, 1987, available at http://www.eas.slu.edu/People/RBHerrmann/getzip.html]. Synthetics are calculated for distances to stations GSMY, ETKA, KIKV, TASE, and GANE. The resulting phase velocity matches the observations in Figure 2.

thus can be justified only by testing the consistency of the seismic data with the model. We use the spectral simplifications as a starting place to explore the link between plume height, volcanic flow in the conduit, and seismic waves. For future studies, infrasound data from large eruptions could potentially be used to provide constraints on the true turbulence spectrum of volcanic jets [e.g., *Matoza et al.*, 2009; *Fee et al.*, 2010].

3.3. Step 3: Relate Single Force to Far-Field Seismic Waves

[22] Finally, we calculate the far-field surface waves resulting from a single force. For a vertical single force F, the displacement amplitude u of a fundamental mode Rayleigh wave with wave number k traveling in a half-space is

$$u = \frac{0.07F}{\mu}\sqrt{\frac{k}{r}}\,e^{-(f\pi/Qc)r}, \tag{6}$$

where μ is the shear modulus, r is the distance from the source, c is the surface wave propagation velocity, and Q is the quality factor for attenuation at frequency, f [*Aki and Richards*, 1980]. Equivalently, equation (6) describes the spectrum of propagating surface waves as a function of wave number k. This relationship is appropriate for a source at the Earth's surface.

[23] Equation (6) is applicable for a single mode. For real data, we apply a narrow band pass that captures multiple modes. Since the modal spectrum is dense near 1 s, it is difficult to analytically add all of the relevant modes together to construct the amplitude. Instead, we generate synthetic seismograms using a wave number-frequency summation method and band pass the synthetics to obtain a correction for the finite band pass (Figure 4) (R. B. Herrmann, Computer programs in seismology, 1987, available at http://www.eas.slu.edu/People/RBHerrmann/getzip.html). Empirically, we find that an impulse source for a given F band passed at 0.67–2 s period at the regional distances studied here produces an amplitude 2.4 times greater than that predicted by equation (6) for a half-space homogeneous velocity model. This correction factor also holds for a more realistic velocity model such as AK135 [*Kennett et al.*, 1995; *Montagner and Kennett*, 1996]. Therefore, we apply this correction factor of 2.4 to our predicted amplitude found using equation (6).

[24] By assuming values for μ, v, and ρ, and intrinsic Q we can calculate ground displacement as a function of column height and observed wave number k. Combining equations (1) with equations (4)–(6) with the finite band-pass correction yields

$$u = \frac{0.17\rho v}{\mu}\sqrt{\frac{k}{r}}\left(\frac{H}{1.67}\right)^{3.86}e^{-(f\pi/Qc)r}, \tag{7}$$

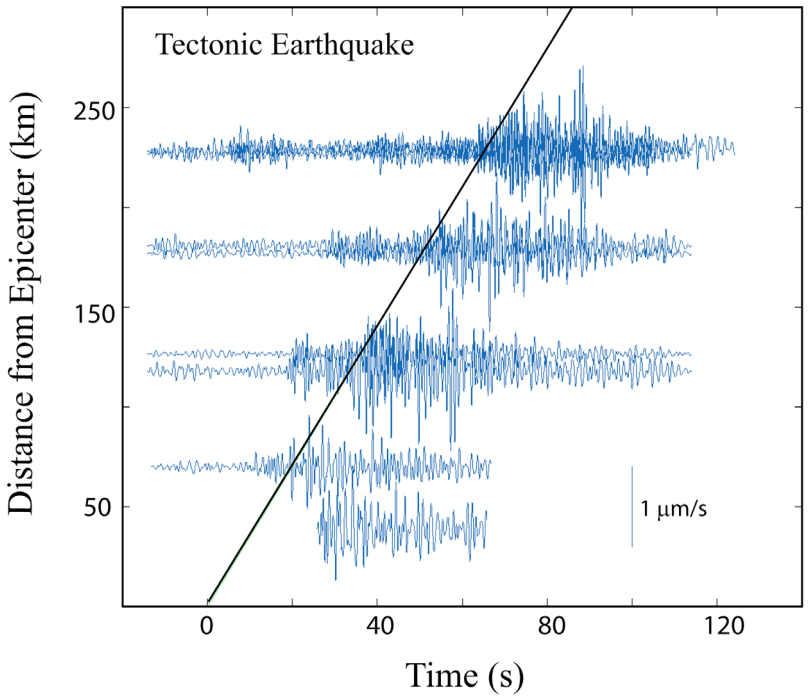

Figure 5. Waveforms for a tectonic earthquake located near Kasatochi Volcano band passed at 0.67–2 s as recorded at stations used in this study. Black line shows arrival of surface waves at c = 3400 m s^{-1}. Coda wave amplitudes in this band are nearly independent of distance.

where H is in km and the other variables are in MKS units. Note that as in equation (1), the constants in equation (7) are not dimensionless.

[25] Equation (7) predicts the amplitude of the seismic waves resulting from a certain column height based entirely on previously established empirical relations and known physics. The column height is an observed quantity and the wave number and epicentral distance r are generally well-resolved for seismic data, as are the dense rock density ρ and the shear modulus μ. We estimate Q in our study area by examining the falloff in surface wave energy amplitudes with distance for propogation velocity, c, at frequency, f. Therefore, utilizing equation (7) requires estimating only one relatively poorly constrained eruptive quantity, the vent velocity v.

[26] A potential complication to this seismic model is the dominance of scattering at high frequencies [e.g., *Wu*, 1985]. We evaluate this possibility by examining the coda waves of two brittle failure earthquakes that occurred near Kasatochi Volcano in the day prior to the eruption (Figure 5). Although locating events in this area is difficult, *Ruppert et al.* [2011] show that these earthquakes likely occurred within 5 km of the volcano. In the 0.67–2 s band pass, coda wave amplitudes of these earthquakes do not decay as observed for the eruptive events (compare to Figure 6). Rather, the coda amplitudes are nearly independent of distance, as might be expected for a highly scattering medium [*Aki and Chouet*, 1975]. The difference between the amplitude decay of the earthquake coda and the eruptive amplitudes suggests that the amplitude of the eruptive phenomena is not dominated by the scattering effect.

3.4. Model Applicability

[27] We now discuss the range of conditions and eruption styles for which this model is appropriate. Because multiple physical processes produce seismic waves at a variety of

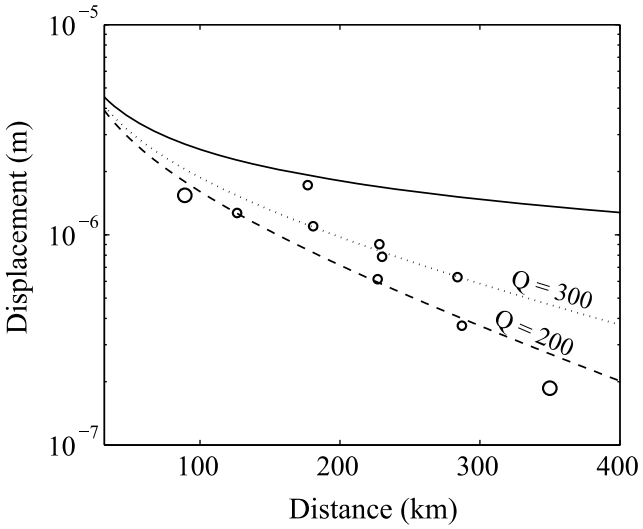

Figure 6. Ground displacement in frequency band analyzed of coeruptive seismicity with distance from Kasatochi Volcano for the largest ash-producing explosion. Large circles are broadband stations ATKA and AMKA. Small circles are short-period stations. Lines show model fit for H = 18 km and v = 120 m s^{-1} for Q of infinity (solid line), Q of 300 (dotted line), and Q of 200 (dashed line).

frequencies during large ash-producing volcanic eruptions, it is sometimes difficult to connect broadband seismic amplitudes with eruptive properties directly, particularly in the near field and for small eruptions. For example, local processes including rockfalls and pyroclastic flows can dominate seismic recordings local to the volcano.

[28] Because the calculated mass ejection rate accounts only for erupted material that provides energy for buoyant ascent of ash-rich plumes, our model is not applicable for phreatic eruptions or eruptive phenomena apart from the plume, such as pyroclastic flows and lava fountaining. In the case of eruptions where the majority of the mass ejected is not entrained in the plume, the model may overestimate plume height for a given amplitude of ground shaking.

[29] The model is also only appropriate for plumes that rise to altitudes of 5 km or higher for two reasons. (1) The empirical regression of *Sparks et al.* [1997] is not constrained for plume heights below 5 km. (2) The assumption that the upward mobility of the plume is thermally driven may not be correct at heights where material can travel ballistically. The maximum ballistic height of a projectile with initial velocity v occurs when the initial kinetic energy equals the gravitational potential energy, i.e., $1/2\ M\ v^2 = Mgh$, where M is mass, g is the acceleration due to gravity, and h is ballistic height. Thus, the maximum ballistic height is $1/2\ v^2/g$. Assuming $v = 300\ m\ s^{-1}$ or less, ballistics could be ejected to 4.5 km height. In the case of small eruptions at the Tungurahua and Santiaguito volcanoes, *Johnson et al.* [2004, 2005] show that amplitudes of coeruptive seismic waves scale poorly with eruption intensity. In both cases, however, eruption plumes analyzed were less than 4 km in height.

[30] This model is also not appropriate in cases where the source of coeruptive volcanic tremor is not the volcanic vent, but elsewhere in the system. For example, during the 2008 eruption of Okmok Volcano, coeruptive tremor amplitude correlated poorly with volcanic plume height after the opening phase of the eruption. *Haney* [2010] estimates that the VLP tremor occurred along the length of a dike at 2 km depth. Thus, in the case of Okmok, Haney concludes that the primary tremor source likely reflected the flux of magma from the shallow magma chamber into the dike rather than mass ejection at the vent directly.

[31] Similarly, we must avoid performing this analysis on time series where the seismic data are dominated by earthquakes sourced from depth. In the case of the Kasatochi eruption, for example, the far-field seismic energy radiated by preeruptive earthquakes was up to 4 times larger in amplitude than the coeruptive tremor at the distances we consider when seismic energy is averaged over 10 min windows. For this reason, we limit our analysis at Kasatochi to a time period free of large earthquakes.

[32] The model is applicable only when the volcanic vent is open and freely emitting material. Therefore, caution must be used when considering the initial stages of eruption. During this time frame, a large portion of the seismic energy may be related to "throat clearing" or removing the lid that caps the magma body. For example, the first large ash-producing explosion during the 2006 eruption of Augustine Volcano produced stronger ground shaking than the subsequent 20 ash-producing explosions, although the plume height of the first explosion was similar to that of many later explosions.

[33] Finally, atmospheric effects should be considered when applying our model. For example, the model is most appropriate for large eruptions with strong plumes where tropospheric wind shear and other atmospheric instabilities are minimal. In addition, because the buoyancy of volcanic ash plumes can increase significantly if atmospheric water vapor is entrained in the plume [*Woods*, 1993; *Tupper et al.*, 2009], our model is more applicable in dry subpolar environments such as Alaska than in moist tropical environments. However, in all environments, atmospheric humidity does not have an appreciable effect on large eruption columns greater than 15 km in height [*Woods*, 1993].

4. Data Analysis and Results

4.1. Kasatochi

[34] To apply our model to the eruption of Kasatochi, we begin by measuring coeruptive ground displacement at short-period and broadband seismometers primarily located west of the volcano. The geometry of the Aleutian Islands provides us with a nearly linear array. We are not able to use data recorded at Great Sitkin Volcano because coeruptive seismic waves are clipped there (Figure 2). We also do not use data east of Atka Island because seismic waves generated by Kasatochi Volcano would likely be contaminated by those generated by the simultaneous eruption of Okmok Volcano, roughly 350 km east of Kasatochi.

[35] This use of far-field data is an advantage because far-field data are not likely to be contaminated by energy radiated from secondary surficial processes. During the Kasatochi eruptions, huge pyroclastic and block and ash flows left the island inundated in up to 15 m of tephra. Secondary seismic sources such as rockfalls and pyroclastic flows decay more quickly with distance than a single force source associated with magma removal because these secondary sources (1) transport a small percentage of mass compared to the total mass ejected, (2) are multipole sources distributed in time and space on the volcano's flank, in contrast to the concentrated single force monopole associated with overall mass ejection [*Kanamori et al.*, 1984, Appendix A], and (3) are largely surficial sources. *Jolly et al.* [2002] show that in the case of Soufriere Hills Volcano, Montserrat, seismic waves generated by pyroclastic flows are highly attenuated ($Q = 20$) due to their surficial travel paths.

[36] We focus our study on the highest amplitude packet of energy radiated by the third and most ash-rich explosion at Kasatochi (2201 UTC, 7 August 2008) (Figure 7), as this explosion began a 16 h phase of continuous venting and is not contaminated by earthquakes. The strongest phase of this energy packet is several minutes in duration and can be clearly identified as it moves out appropriately with distance away from Kasatochi (Figure 2). To select the best possible data set, we examine seismic data from regional brittle failure earthquakes at all Aleutian seismometers. Stations which have unusually strong noise, artificial spectral banding, or poor response in our frequency band of interest are not used. All data analyzed have a signal-to-noise ratio of 2.5 or better in our band of interest. With the exception of

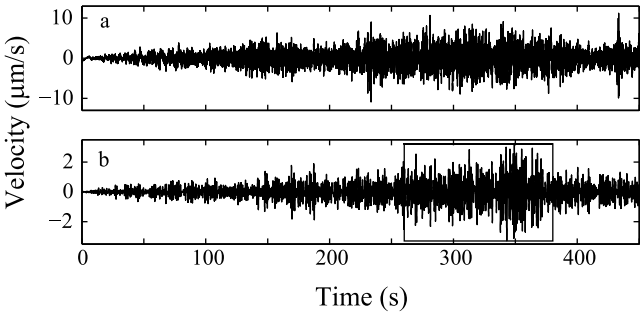

Figure 7. (a) Raw waveform of third large ash-producing explosion of Kasatochi as recorded at short-period station TASE at Tanaga Volcano, 177 km from Kasatochi. (b) Record from Figure 7a band-pass filtered between 0.67 and 2 s. Box shows 2 min window used in computing average peak amplitude.

data from the two short-period instruments on Semisopochnoi Volcano (Figure 1), data analyzed have a signal-to-noise ratio that is significantly higher than this threshold. We retain these stations in the analysis, however, as they are helpful in estimating Q. Stations analyzed are shown in Figure 1.

[37] Once appropriate data are selected, we correct for instrument response and band-pass filter data between 0.67 and 2 s (Figure 7). We choose this frequency range because it is well within the response range of short-period instruments, yet it is below the frequency range generally radiated by pyroclastic flows [e.g., *Zobin et al.*, 2009]. Although site effects are still a problem at frequencies near 1 Hz, we find that measurements made in higher-frequency bands have significantly increased scatter. After filtering data, we select a 2 min duration window which contains the maximum amplitudes (Figure 7). We measure the peak amplitude in 2 s time bins over the window. We then take the L2 norm of this distribution to find a time-averaged peak amplitude of surface wave energy radiated coeruptively.

[38] Figure 6 shows that the relative amplitude of the observed seismic waves fall off with distance. Scatter in measurements likely results from unmodeled site effects. Our measurements are generally consistent with Q values of 200–300. This range is slightly high relative to standard attenuation models (e.g., shallow Qp = 180, Qs = 85 [*Montagner and Kennett*, 1996]) but still reasonable for intact oceanic crust. The observed amplitude falloff with distance is a helpful corroboration of the direct Rayleigh wave interpretation of the coeruptive seismicity in equation (6). The observation is consistent with other studies of vulcanian eruptions that show that seismic energy radiated coeruptively is dominated by Rayleigh waves [*McNutt*, 1994b].

[39] To evaluate the fit of our model, we calculate the range of plume heights, H, predicted for a reasonable range of v, given the measured displacement, u. We assume a shear modulus of $\mu = 3 \times 10^{10}$ Pa and specify $k = 2\pi f/c$, where the frequency in the middle of the observed band pass $f = 1$ s and $c = 3.4 \times 10^3$ m s^{-1}. Dense rock equivalent, ρ, is 2700 kg m^{-3}. We then compare predicted plume heights to the observed maximum plume height of 18 km [*Waythomas et al.*, 2010].

[40] Figure 8 shows that in the case of Kasatochi, for a wide range of reasonable values of v, we predict H of 13–20 km. Thus, the observed H of 18 km is well within the range of those values predicted by our model. In Figure 8, H of 18 km corresponds to v of 120 m s^{-1}. Figure 6 shows ground displacement measurements for the Kasatochi eruption and predicted ground displacement with distance in our preferred model, where v = 120 m s^{-1}, H is 18 km, and Q is between 200 (Figure 8, dashed line) and 300 (Figure 8, dotted line). Because our preferred velocity based on analysis of ~1 s data is in the range of v predicted by laboratory studies of volcanic columns [*Kieffer and Sturtevant*, 1984] and observational estimates [*McNutt and Nishimura*, 2008], Kasatochi eruption data appear to be consistent with the flat spectrum source model as proposed above. Alternatively, if the true v is larger than 120 m s^{-1}, as is possible for an eruption as large and violent as the Kasatochi eruption, the data may accommodate an increase in spectral amplitude of the source with increasing period as would be expected from turbulence models [*Kolmogorov*, 1991; *Mathieu and Scott*, 2000; *Matoza et al.*, 2009] and *Mastin*'s [2007] Plumeria model. We also note that large pyroclastic flows occurred during the Kasatochi eruption [*Waythomas et al.*, 2010; *Scott et al.*, 2010]. If a significant portion of the ejected mass is not contributing to the thermal buoyancy of the plume, as we assume, it is possible that we are overestimating v by using equation (7).

[41] Errors in measured plume height are not reported in the literature for the Kasatochi eruption. However, *Mastin et al.* [2009] estimate errors in relating H to M on the basis of reasonably well-constrained eruption source parameters from a number of other eruptions. In the case of the Kasa-

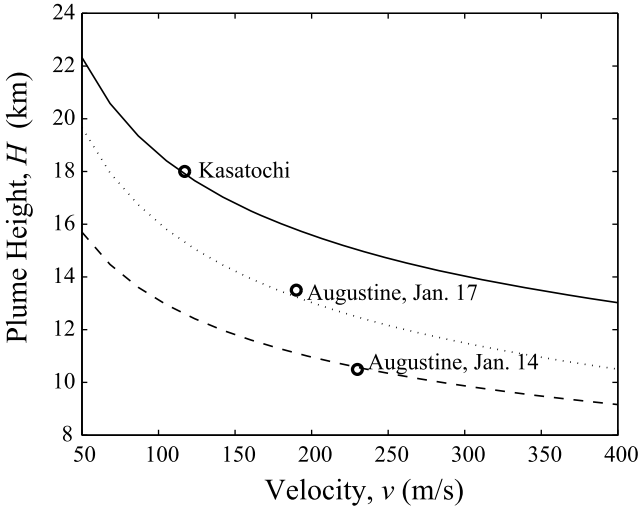

Figure 8. Calculated plume heights, H, for a possible range in v given measured displacement, u, for explosions at Kasatochi Volcano on 8 August 2008 (solid line), Augustine Volcano on 14 January 2006 (dashed line), and Augustine Volcano on 17 January 2006 (dotted line). Observed plume heights, H, and inferred preferred velocities, v, are indicated by circles.

tochi eruption, we calculate $\dot{M} = 2.6 \times 10^7$ kg s^{-1} using equation (1). *Mastin et al.* [2009] find that the 50% confidence interval for this $\dot{M}$ includes plume heights of ~18 km ± 4 km. Scatter observed in the H to $\dot{M}$ relation results from error in H estimates, errors in eruptive volume estimates, and unmodeled effects of pyroclastic flows and water vapor entrainment into the plume.

4.2. Augustine

[42] To investigate the robustness of the model in a different eruptive setting, we tested its applicability to the 2006 eruption of Augustine volcano. Although Augustine is locally instrumented, for our analysis we use the short-period seismometer OPT located 37 km from the erupting vent. This is required, since our model uses far-field surface waves and because we do not want the tephra ejection signal contaminated by more surficial local processes that dominate the short-period signals on the island, such as rockfalls and pyroclastic flows. In the case of the 2006 eruption of Augustine, *McNutt et al.* [2010] showed that pyroclastic flows were visible seismically only on stations near the flow travel path and not on the volcano flanks opposite the flow path.

[43] We process Augustine data in a manner identical to that described for Kasatochi data. Figure 8 shows calculated plume heights for a range of v for explosions at 0140 UTC on 14 January 2006 and 1657 UTC on 17 January 2006, which had maximum plume heights of 10.5 and 13.5 km above sea level, respectively, on the basis of radar and pilot reports [*Power and Lalla*, 2010]. The far-field short-period amplitudes of these two explosions are similar to other explosions in the sequence (with the exception of the initial 11 January 2006 explosion). We selected these explosions to analyze because they are representative of the entire eruption. Because the initial explosions from the 2006 eruption of Augustine volcano may have included energy from the brittle failure vent-clearing processes, we do not analyze data from 11 January 2006. In the case of Augustine, the volcanic vent is well above sea level at ~1260 m altitude. Thus, when applying our model, we correct for the difference between vent altitude and the reported plume heights, which are defined with respect to sea level.

[44] As in the Kasatochi case, we assume a shear modulus of $\mu = 3 \times 10^{10}$ Pa and specify $k = 2\pi f/c$, where the observed frequency is $f = 1$ s and $c = 3.4 \times 10^3$ m s^{-1}. Dense rock equivalent, ρ, is 2700 kg m^{-3}. In the case of the 17 January 2006 explosion, for v ranging from 50 to 400 m s^{-1}, we predict H of 11–18 km. In the case of the 14 January 2006 explosion, we predict H of 9–15 km. Thus, the observed H of 13.5 km and 10.5 km for the 17 January and 14 January plumes, respectively, are well within the range of plume heights predicted by our model. Our preferred models, which fit the data shown in Figure 8, require v of 190 m s^{-1} and 230 m s^{-1} for the 17 January and 14 January explosions, respectively. These values are similar to the range of v calculated by *Caplan-Auerbach et al.* [2010] on the basis of infrasound data. As in the Kasatochi case, we lack error estimates in measured H for the Augustine eruptions studied. Following *Mastin et al.* [2009], however, we expect errors in relating H to $\dot{M}$ to be roughly 3 km for the 10.5 km plume and 4 km for the 13.5 km plume for the 50% confidence interval.

5. Dynamical Implications

[45] Because the observed H is within the range of the modeled H considering unknowns in v, the single-force model may be an appropriate force system in the case of the two eruptions we consider. The most surprising aspect of the model's success is the fact that we can relate plume height to seismic wave amplitude using ~1 s radiated waves assuming a reasonable range of v (120–230 m s^{-1}) in our preferred models. This consistency implies that the high-frequency fluctuations of the plume are comparable in magnitude to the long-period eddies. We cannot rule out the possibility that our preferred v estimates are lower than in reality, in which case the source spectral amplitude may be decreasing with frequency in contrast to the flat spectrum we assume. That scenario would not be unexpected, as turbulent flows commonly have stronger eddies at long periods than at short periods [*Kolmogorov*, 1991; *Mathieu and Scott*, 2000; *Fee et al.*, 2010]. However, the spectrum can be modified by additional processes such as supersonic flow [*Smits and Dussauge*, 2006].

[46] The appropriateness of these spectral models cannot be tested independently, as there are not currently any other means to sample the time-dependent velocity distribution in the core of an opaque, large-scale volcanic jet. Some other methods are being developed. For instance, the length scale of turbulent eddies in a volcanic plume has recently been measured in plumes on the basis of photographs [*Andrews and Gardner*, 2009], and infrasound is being used to track vent velocities [*Caplan-Auerbach et al.*, 2010]. However, none of these methods have been used to infer a spectrum of velocities. Seismic data are intrinsically sensitive to a different region of the plume than other methods. Photographs and infrasonic methods are more sensitive to the outer sheath of the jet that is well-coupled to the atmosphere, whereas seismic data record fluctuations as coupled to the ground, i.e., inside the vent.

[47] Given these complications, perhaps the best way to assess the validity of the model proposed here is to compare the values of v inferred from equation (7) for a large suite of eruptions. If v is physically reasonable and consistent across eruptions, then the simple source model is consistent with the data. A similar line of reasoning has been used with great success in assessing the values of earthquake source parameters, such as rupture velocity [*Kanamori and Anderson*, 1975]. The seismic measurements presented in this paper are a first step toward assembling this data set. They suggest that future work on the seismic source spectrum of plumes would be a fruitful avenue into examining the fluid dynamics of erupting jets.

6. Practical Implications

[48] For the Aleutian Islands and many other remote volcanoes in the North Pacific, the primary safety concern is the threat of ash clouds to aircraft. Airlines are most concerned about ash clouds that reach aircraft cruising altitudes. Estimating volcanic plume heights in remote environments in real time (and even in retrospect) is always

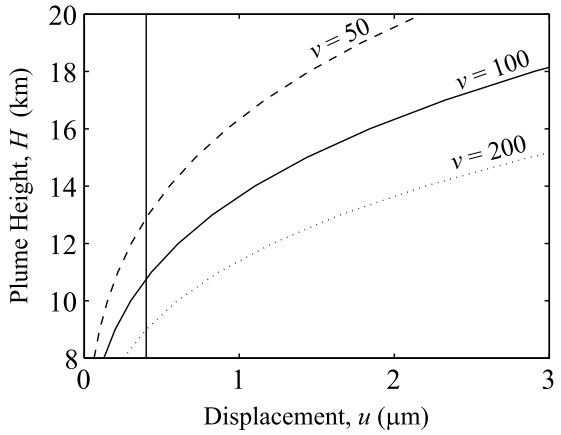

Figure 9. Expected ground displacement at 1 s period due to a plume observed at Great Sitkin, 40 km distant from Kasatochi, for three vent velocities: 50 m s^{-1} (dashed), 100 m s^{-1} (solid), and 200 m s^{-1} (dotted). Vertical line indicates conservative noise level at Great Sitkin seismic stations.

challenging, particularly when clouds are obscuring activity and the timing of satellite passes is not optimal. With further development, this model could potentially be used to constrain plume heights in near real time. In the case of the Kasatochi eruption, we would have estimated plume heights of 13–20 km using our model on the basis of seismic data alone, potentially giving airlines notice that the eruption was large enough to be dangerous. To narrow this range in height, we would need more accurate estimates of v through other data sources such as infrasound, radar, or a larger empirical database of v measurements from similar eruptions.

[49] To illustrate the potential utility of the approach, we examine our ability to characterize future eruptions at Kasatochi Volcano using the nearest seismic stations, incorporating some of the uncertainty in the one free parameter, v. Figure 9 shows calculated ground displacement at Great Sitkin stations estimated for eruptions of Kasatochi using a variety of reasonable v values. We assume a detection threshold of 0.4 μm, as AVO short-period seismometers in the Aleutian Arc often have noise below this threshold for raw unfiltered data. This is a conservative estimate for eruption detection, provided the recording environment is relatively quiet and the seismometers are functioning optimally. Figure 9 shows that generally we can expect to detect coeruption seismicity for explosive eruptions with plumes that reach 9–12 km height above sea level or higher at Kasatochi Volcano. Discriminating the source of seismic energy, as discussed in section 3.4, may remain a challenge, however.

[50] This same approach allows us to estimate detection capability for eruptions at other unmonitored volcanoes. For instance, Bogoslof and Seguam volcanoes are small, unmonitored Aleutian Islands, such as Kasatochi (Figure 1). Bogoslof most recently erupted in 1992 and had seven additional historic eruptions. Seguam most recently erupted in 1993 and had five additional historic eruptions. The nearest seismometers to Bogoslof and Seguam are those of the Okmok and Korovin seismic networks, respectively, ~50 km and ~100 km distant. Using Figure 10, we estimate that large, continuous, ash-producing eruptions at Bogoslof and Seguam could be visible in high-frequency data at the nearest seismic stations if the plumes reached roughly 8 and 9 km, respectively, in altitude for v = 300 m s^{-1} and 13 and 15 km, respectively, in altitude if v = 50 m s^{-1}. Again, a reasonable variation in v (50–300 m s^{-1}) leads to scatter in predicted plume heights over a 4 km range.

[51] Our model could potentially provide plume height estimates within 4 km independent of remote sensing techniques that could be considered along with estimates from other sources. To do this, more work is needed to constrain errors, develop improved source models, explore applicability to different eruptions, and test velocity model assumptions. Another consideration is that several physical processes cause seismic tremor in the Earth's crust, so other data are needed to confirm that tremor observed is coeruptive tremor before applying our model. Uncertainties in tremor source process would likely lead to far more false positives than false negatives. Thus our model could be used as a conservative indicator of threats to aviation from volcanic ash.

7. Conclusions

[52] Our model is generally successful in relating plume height to ground shaking in the 2008 eruption of Kasatochi Volcano and the 2006 eruption of Augustine Volcano for reasonable values of the one unknown parameter, v. This suggests that using plume height to calculate the mass ejection rate and interpreting the resulting force system as a single force may be appropriate techniques. The single force model appropriate at low frequencies also fits measurements of Rayleigh waves reasonably well at frequencies of ~1 s. This surprising observation suggests that force resulting from the high-frequency turbulence in volcanic jets can be a useful indicator of plume height.

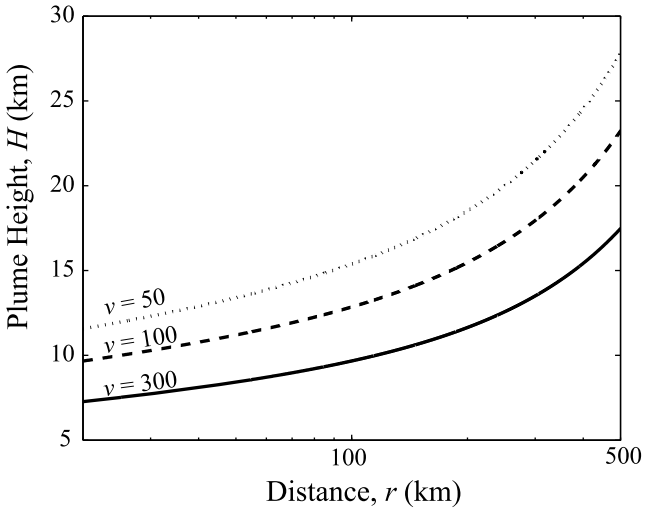

Figure 10. Minimum detectable plume heights with distance calculated using our model, assuming a conservative detection threshold of 0.4e-6 m at 1 s period and vent velocities of 50 m s^{-1} (dotted), 100 m s^{-1} (dashed), and 300 m s^{-1} (solid).

[53] The success and applicability of the model to other vulcanian and plinian eruptions globally remain to be evaluated. However, the results from Kasatochi and Augustine volcanoes are sufficiently encouraging that more work in this field is warranted. Future studies should focus on other eruptions to explore errors and the range of applicability of the model, consider more complicated velocity structures and indirect wave arrivals, consider atmospheric effects, and further investigate frequency variations in energy radiated by the volcanic jet. Further development of this model may give us a means to better understand the relationship of ground shaking to plume height and explore eruption dynamics of the turbulent jet. In the best case scenario, this avenue of research may lead us to constraining plume height on the basis of seismic wave amplitudes in near real time. To reach that goal, calibration with a larger suite of eruptions and a better understanding of the full spectrum of radiated seismic energy are required.

Notation

A area of the vent, m^2.
c surface wave propagation velocity, m s^{-1}.
c_p heat capacity, kJ kg^{-1} K^{-1}.
E thermal energy, J.
F vertical single force, N.
f frequency, Hz.
g acceleration due to gravity, m s^{-2}.
H eruption column or plume height above the vent, km.
h maximum height of ballistics, m.
k wave number, m^{-1}.
$\dot{M}$ mass, kg.
M mass ejection rate, kg s^{-1}.
μ shear modulus, GPa.
ρ density of solid rock, kg m^{-3}.
q dense rock equivalent volumetric ejection rate, m^3 s^{-1}.
Q attenuation quality factor, dimensionless.
S energy spectrum, m^3 s^{-2}.
r distance from source to receiver, m.
τ duration of mass ejection at volcanic vent, s.
ΔT temperature difference between plume and ambient air, K.
u ground displacement, m.
v velocity of material exiting the vent, m s^{-1}.

[54] **Acknowledgments.** Reviews by Larry Mastin, Darcy Ogden, David Schneider, David Hill, David Fee, and two anonymous reviewers significantly improved this manuscript. Seismic stations used in this study were originally installed with funding from the Federal Aviation Administration and are maintained by the Alaska Volcano Observatory, the Alaska Earthquake Information Center, and the Alaska Tsunami Warning Center.

References

Aki, K., and B. Chouet (1975), Origin of coda waves: Source, attenuation, and scattering effects, *J. Geophys. Res.*, *80*, 3322–3342, doi:10.1029/JB080i023p03322.

Aki, K., and P. G. Richards (1980), *Quantitative Seismology: Theory and Methods*, 913 pp., W. H. Freeman, San Francisco, Calif.

Andrews, B. J., and J. E. Gardner (2009), Turbulent dynamics of the 18 May 1980 Mount St. Helens eruption column, *Geology*, *37*, 895–898, doi:10.1130/G30168A.1.

Arnoult, K. M., J. V. Olson, C. A. L. Szuberla, S. R. McNutt, M. A. Garcés, D. Fee, and M. A. H. Hedlin (2010), Infrasound observations of the 2008 explosive eruptions of Okmok and Kasatochi volcanoes, Alaska, *J. Geophys. Res.*, *115*, D00L15, doi:10.1029/2010JD013987.

Brodsky, E. E., H. Kanamori, and B. Sturtevant (1999), A seismically constrained mass discharge rate for the initiation of the May 18, 1980 Mount St. Helens eruption, *J. Geophys. Res.*, *104*, 29,387–29,400, doi:10.1029/1999JB900308.

Caplan-Auerbach, J., A. Bellesiles, and J. K. Fernandes (2010), Estimates of eruption velocity and plume height from infrasonic recordings of the 2006 eruption of Augustine volcano, Alaska, *J. Volcanol. Geotherm. Res.*, *189*, 12–18, doi:10.1016/j.jvolgeores.2009.10.002.

Carey, S., and H. Sigurdsson (1989), The intensity of plinian eruptions, *Bull. Volcanol.*, *51*, 28–40, doi:10.1007/BF01086759.

Chouet, B. A. (1996), Long-period volcano seismicity: Its source and use in eruption forecasting, *Nature*, *380*, 309–316, doi:10.1038/380309a0.

Chouet, B., P. Dawson, T. Ohminato, M. Martini, G. Saccorotti, F. Giudicepietro, G. De Luca, G. Milana, and R. Scarpa (2003), Source mechanisms of explosions at Stromboli Volcano, Italy, determined from moment-tensor inversions of very-long-period data, *J. Geophys. Res.*, *108*(b1), 2019, doi:10.1029/2002JB001919.

Chouet, B., P. Dawson, and A. Arciniega-Ceballos (2005), Source mechanism of vulcanian degassing at Popocatepetl Volcano, Mexico, determined from waveform inversions of very long period signals, *J. Geophys. Res.*, *110*, B07301, doi:10.1029/2004JB003524.

Chouet, B. P., P. Dawson, and M. Martini (2008), Shallow-conduit dynamics at Stromboli Volcano, Italy, imaged from waveform inversions, *Geol. Soc. Spec. Publ.*, *307*, 57–84, doi:10.1144/SP307.5.

Chouet, B., P. Dawson, M. James, and S. Lane (2010), Seismic source mechanism of degassing bursts at Kilauea Volcano, Hawaii: Results from waveform inversion in the 10–150 s band, *J. Geophys. Res.*, *115*, B09311, doi:10.1029/2009JB006661.

Fee, D., A. Stefke, and M. Garces (2010), Characterization of the 2008 Kasatochi and Okmok eruptions using remote infrasound arrays, *J. Geophys. Res.*, *115*, D00L10, doi:10.1029/2009JD013621.

Haney, M. M. (2010), Location and mechanism of very long period tremor during the 2008 eruption of Okmok volcano from interstation arrival times, *J. Geophys. Res.*, *115*, B00B05, doi:10.1029/2010JB007440.

Johnson, J. B., A. J. L. Harris, S. T. M. Sahetapy-Engel, R. Wolf, and W. I. Rose (2004), Explosion dynamics of pyroclastic eruptions at Santiaguito volcano, *Geophys. Res. Lett.*, *31*, L06610, doi:10.1029/2003GL019079.

Johnson, J. B., M. C. Ruiz, J. M. Lees, and P. Ramon (2005), Poor scaling between elastic energy release and eruption intensity at Tungurahua volcano, Ecuador, *Geophys. Res. Lett.*, *32*, L15304, doi:10.1029/2005GL022847.

Jolly, A. D., G. Thompson, and G. E. Norton (2002), Locating pyroclastic flows on Soufriere Hills volcano, Montserrat, West Indies, using amplitude signals from high dynamic range instruments, *J. Volcanol. Geotherm. Res.*, *118*, 299–317, doi:10.1016/S0377-0273(02)00299-8.

Kanamori, H., and D. L. Anderson (1975), Theoretical basis of some empirical relations in seismology, *Bull. Seismol. Soc. Am.*, *65*, 1073–1095.

Kanamori, H., and J. W. Given (1982), Analysis of long-period seismic waves excited by the May 18, 1980, eruption of Mount St. Helens: A terrestrial monopole?, *J. Geophys. Res.*, *87*, 5422–5432, doi:10.1029/JB087iB07p05422.

Kanamori, H., J. W. Given, and T. Lay (1984), Analysis of seismic body waves excite by the Mount St. Helens eruption of May 18, 1980, *J. Geophys. Res.*, *89*, 1856–1866, doi:10.1029/JB089iB03p01856.

Kennett, B. L. N., E. R. Engdahl, and R. Buland (1995), Constraints on seismic velocities in the Earth from travel times, *Geophys. J. Int.*, *122*, 108–124, doi:10.1111/j.1365-246X.1995.tb03540.x.

Kieffer, S. W. (1981), Fluid dynamics of the May 18, 1980 blast at Mt. St. Helens, *U.S. Geol. Surv. Prof. Pap.*, *1250*, 379–400.

Kieffer, S. W., and B. Sturtevant (1984), Laboratory studies of volcanic jets, *J. Geophys. Res.*, *89*, 8253–8268, doi:10.1029/JB089iB10p08253.

Kolmogorov, A. N. (1991), The local structure of turbulence in incompressible viscous fluid for very large Reynolds numbers, *Proc. R. Soc. London, Ser. A*, *434*, 9–13, doi:10.1098/rspa.1991.0075.

Mastin, L. G. (2007), A user-friendly one-dimensional model for wet volcanic plumes, *Geochem. Geophys. Geosyst.*, *8*, Q03014, doi:10.1029/2006GC001455.

Mastin, L. G., et al. (2009), A multidisciplinary effort to assign realistic source parameters to models of volcanic ash-cloud transport and dispersion during eruptions, *J. Volcanol. Geotherm. Res.*, *186*, 10–21, doi:10.1016/j.jvolgeores.2009.01.008.

Mathieu, J., and J. Scott (2000), *An Introduction to Turbulent Flow*, Cambridge Univ. Press, Cambridge, U. K.

Matoza, R. S., D. Fee, M. A. Garcés, J. M. Seiner, P. A. Ramón, and M. A. H. Hedlin (2009), Infrasonic jet noise from volcanic eruptions, *Geophys. Res. Lett.*, *36*, L08303, doi:10.1029/2008GL036486.

McNutt, S. R. (1994a), Volcanic tremor amplitude correlated with eruption explosivity and its potential use in determining ash hazards to aviation, *U.S. Geol. Surv. Bull.*, *2047*, 377–385.

McNutt, S. R. (1994b), Volcanic tremor from around the world: 1992 update, *Acta Vulcanol.*, *5*, 197–200.
McNutt, S. R. (2005), Volcanic seismicity, *Annu. Rev. Earth Planet. Sci.*, *33*, 461–491, doi:10.1146/annurev.earth.33.092203.122459.
McNutt, S. R., and T. Nishimura (2008), Volcanic tremor during eruptions: Temporal characteristics, scaling an constraints on conduit size and process, *J. Volcanol. Geotherm. Res.*, *178*, 10–18, doi:10.1016/j.jvolgeores.2008.03.010.
McNutt, S. R., G. Tytgat, S. A. Estes, and S. D. Stihler (2010), A parametric study of the January 2006 explosive eruptions of Augustine Volcano, using seismic, infrasonic, and lightning data, in *The 2006 Eruption of Augustine Volcano, Alaska*, edited by J. A. Power, M. L. Coombs, and J. T. Freymueller, *U.S. Geol. Surv. Prof. Pap.*, *1769*, 85–102.
Montagner, J.-P., and B. L. N. Kennett (1996), How to reconcile body-wave and normal-mode reference Earth models?, *Geophys. J. Int.*, *125*, 229–248, doi:10.1111/j.1365-246X.1996.tb06548.x.
Morton, B. R., G. I. Taylor, and J. S. Turner (1956), Gravitational turbulent convection from maintained and instantaneous sources, *Proc. R. Soc. London, Ser. A*, *234*, 1–23, doi:10.1098/rspa.1956.0011.
Nishimura, T. (1995), Source parameters of the volcanic eruption earthquakes at Mount Takachi, Hokkaido, Japan, and a magma ascending model, *J. Geophys. Res.*, *100*, 12,465–12,474, doi:10.1029/95JB00867.
Nishimura, T., and H. Hamaguchi (1993), Scaling law of volcanic explosion earthquake, *Geophys. Res. Lett.*, *20*, 2479–2482, doi:10.1029/93GL02793.
Ogden, D. E., G. A. Glatzmaier, and K. H. Wohletz (2008), Effects of vent overpressure on buoyant eruption columns: Implications for plume stability, *Earth Planet. Sci. Lett.*, *268*(3–4), 283–292, doi:10.1016/j.epsl.2008.01.014.
Ohminato, T., M. Takeo, H. Kumagai, T. Yamashina, J. Oikawa, E. Koyama, H. Tsuji, and T. Urabe (2006), Vulcanian eruptions with dominant single force components observed during the Asama 2004 volcanic activity in Japan, *Earth Planets Space*, *58*, 583–593.
Omori, F. (1911), The Usa-San eruption and earthquake elevation phenomena, *Bull. Imp. Earthquake Invest. Comm.*, *5*, 1–38.
Papale, P., and A. Longo (2008), Vent conditions for expected eruptions at Vesuvius, *J. Volcanol. Geotherm. Res.*, *178*, 359–365, doi:10.1016/j.jvolgeores.2008.05.012.
Power, J. A., and D. J. Lalla (2010), Seismic observations of Augustine Volcano, 1970–2007, in *The 2006 Eruption of Augustine Volcano, Alaska*, edited by J. A. Power, M. L. Coombs, and J. T. Freymueller, *U.S. Geol. Surv. Prof. Pap.*, *1769*, 3–40.
Rudinger, G. (1980), *Fundamentals of Gas-Particle Flow*, Elsevier, New York.
Ruppert, N. A., S. Prejean, and R. A. Hansen (2011), Seismic swarm associated with the 2008 eruption of Kasatochi Volcano, Alaska: Earthquake locations and source parameters, *J. Geophys. Res.*, doi:10.1029/2010JB007435, in press.
Scott, W. E., C. J. Nye, C. F. Waythomas, and C. A. Neal (2010), August 2008 eruption of Kasatochi volcano, Aleutian Islands, Alaska: Resetting an island landscape, *Arct. Antarct. Alp. Res.*, *42*, 250–259, doi:10.1657/1938-4246-42.3.250.
Smits, A., and J.-P. Dussauge (2006), *Turbulent Shear Layers in Supersonic Flow*, 2nd ed., Springer, New York.
Sparks, R. S. J., M. I. Bursik, S. N. Carey, J. S. Gilbert, L. S. Glaze, H. Sigurdsson, and A. W. Woods (1997), *Volcanic Plumes*, John Wiley, New York.
Thompson, P. A. (1972), *Compressible-Fluid Dynamics*, McGraw-Hill, New York.
Tupper, A., C. Textor, M. Herzog, H.-F. Graf, and M. S. Richards (2009), Tall clouds from small eruptions: The sensitivity of eruption height and fine ash content to tropospheric instability, *Nat. Hazards*, *51*, 375–401, doi:10.1007/s11069-009-9433-9.
Uhira, K., and M. Takeo (1994), The source of explosive eruptions of Sakurajima volcano, Japan, *J. Geophys. Res.*, *99*, 17,775–17,789, doi:10.1029/94JB00990.
Waythomas, C. F., W. E. Scott, S. G. Prejean, D. J. Schneider, P. Izbekov, and C. J. Nye (2010), The 7–8 August 2008 eruption of Kasatochi Volcano, central Aleutian Islands, Alaska, *J. Geophys. Res.*, *115*, B00B06, doi:10.1029/2010JB007437.
Wilson, L., R. S. L. Sparks, T. C. Huang, and N. D. Watkins (1978), The control of volcanic eruption column heights by eruption energetics and dynamics, *J. Geophys. Res.*, *83*, 1829–1836, doi:10.1029/JB083iB04p01829.
Woods, A. W. (1993), Moist convection and injection of volcanic ash into the atmosphere, *J. Geophys. Res.*, *98*, 17,627–17,636, doi:10.1029/93JB00718.
Woods, A. W. (1995), The dynamics of explosive volcanic eruptions, *Rev. Geophys.*, *33*, 495–530, doi:10.1029/95RG02096.
Wu, R. (1985), Multiple-scattering and energy-transfer of seismic waves separation of scattering effect from intrinsic attenuation: 1. Theoretical modeling, *Geophys. J. R. Astron. Soc.*, *82*, 57–80.
Zobin, V. M., I. Plascencia, G. Reyes, and C. Navarro (2009), The characteristics of seismic signals produced by lahars and pyroclastic flows: Volcan de Colima, Mexico, *J. Volcanol. Geotherm. Res.*, *179*, 157–167, doi:10.1016/j.jvolgeores.2008.11.001.

E. E. Brodsky, Department of Earth and Planetary Sciences, University of California, 1156 High St., Santa Cruz, CA 95064, USA.
S. G. Prejean, U.S. Geological Survey, Alaska Volcano Observatory, 4210 University Ave., Anchorage, AK 99508, USA. (sprejean@usgs.gov)